

Persistence of the Gleissberg 88-year solar cycle over the last ~12,000 years: Evidence from cosmogenic isotopes

Alexei N. Peristykh¹ and Paul E. Damon

Department of Geosciences, University of Arizona, Tucson, Arizona, USA

Received 15 March 2002; revised 2 July 2002; accepted 9 July 2002; published 3 January 2003.

[1] Among other longer-than-22-year periods in Fourier spectra of various solar–terrestrial records, the 88-year cycle is unique, because it can be directly linked to the cyclic activity of sunspot formation. Variations of amplitude as well as of period of the Schwabe 11-year cycle of sunspot activity have actually been known for a long time and a ca. 80-year cycle was detected in those variations. Manifestations of such secular periodic processes were reported in a broad variety of solar, solar–terrestrial, and terrestrial climatic phenomena. Confirmation of the existence of the Gleissberg cycle in long solar–terrestrial records as well as the question of its stability is of great significance for solar dynamo theories. For that perspective, we examined the longest detailed cosmogenic isotope record—INTCAL98 calibration record of atmospheric ¹⁴C abundance. The most detailed precisely dated part of the record extends back to ~11,854 years B.P. During this whole period, the Gleissberg cycle in ¹⁴C concentration has a period of 87.8 years and an average amplitude of ~1‰ (in $\Delta^{14}\text{C}$ units). Spectral analysis indicates in frequency domain by sidebands of the combination tones at periods of $\approx 91.5 \pm 0.1$ and $\approx 84.6 \pm 0.1$ years that the amplitude of the Gleissberg cycle appears to be modulated by other long-term quasiperiodic process of timescale ~2000 years. This is confirmed directly in time domain by bandpass filtering and time–frequency analysis of the record. Also, there is additional evidence in the frequency domain for the modulation of the Gleissberg cycle by other millennial scale processes. Attempts have been made to explain 20th century global warming exclusively by the component of irradiance variation associated with the Gleissberg cycle. These attempts fail, because they require unacceptably great solar forcing and are incompatible with the paleoclimatic records. *INDEX TERMS:* 7536 Solar Physics, Astrophysics, and Astronomy: Solar activity cycle (2162); 7537 Solar Physics, Astrophysics, and Astronomy: Solar and stellar variability; 2104 Interplanetary Physics: Cosmic rays; 1650 Global Change: Solar variability; *KEYWORDS:* stellar variability, solar dynamo, Gleissberg cycle, cosmic rays, cosmogenic isotopes, global change

Citation: Peristykh, A. N., and P. E. Damon, Persistence of the Gleissberg 88-year solar cycle over the last ~12,000 years: Evidence from cosmogenic isotopes, *J. Geophys. Res.*, 108(A1), 1003, doi:10.1029/2002JA009390, 2003.

1. Introduction

[2] Although there are other century-scale periodicities in cosmogenic isotope variations that have been related to solar activity [Sonett, 1984; Sonett and Finney, 1990; Damon and Sonett, 1991] the first to be clearly established as of solar origin was the Gleissberg cycle. It was shown to be intrinsically related to features of the Schwabe cycle.

[3] The famous “11-year” or Schwabe cycle in the processes of emerging, evolving and disappearance of sunspots and their groups on the solar disk has been long known since its discovery by C. Horrebow in 1770s and

rediscovery by H. Schwabe in 1843 [Vitinskii, 1965]. But it was always clear that the phenomenon in question was in no way strictly a perfect cyclic process. According to Eddy [1977], “a number of subsidiary features of the sunspot cycle have long been noted: times of rise to maxima are generally shorter than times of fall; heights of maxima sometimes alternate in strength from cycle to cycle; amplitudes of maxima, taken in the long term, seem to follow a longer period of seven or eight 11-year cycles, as first noted by Wolf [1862] and later elaborated by Gleissberg [1944]”.

[4] According to an account given by Gleissberg [1958], in 1862 R. Wolf, after completing the first continuous record of the relative sunspot numbers (also-called Wolf-Wolfer or just Wolf numbers), “concluded from the sunspot observations available at that time that high and low maxima did not follow one another at random: a succession of two or three strong maxima seemed to alternate with a succession of two or three weak maxima”. That observation

¹Formerly at Laboratory of Nuclear Space Physics, Division of Plasma Physics, Atomic Physics, and Astrophysics, A. F. Ioffe Physico-Technical Institute, St. Petersburg, Russia.

lead to the suggestion of the existence of a long cycle, or secular variation, the length of which was estimated at that time to be equal to 55 years. Following this earlier work, a ca. 80-year cycle was detected by *Gleissberg* [1958, 1965] in both height and length of the 11-year sunspot cycle by applying a lowpass filtering procedure, which he named “secular smoothing” [*Gleissberg*, 1944], to Wolf number series. Applying that procedure to a gradually enlarged record he calculated and regularly published secularly smoothed epochs and ordinates of maxima and minima of Schwabe cycle in Wolf sunspot numbers [*Gleissberg*, 1944, 1958, 1967, 1976] and for those in frequency of aurorae sightings [*Gleissberg*, 1958, 1965, 1966, 1976].

[5] Reconstruction of epochs of maxima and minima of the frequency of aurorae sightings by *Schove* [1955], that tightly follows the sunspot cycle, allowed tracing the behavior of the Gleissberg cycle for 135 Schwabe cycles back to the 4th century A.D. [*Gleissberg*, 1958]. That time span displayed 19 complete periods of the Gleissberg cycle, inferring the length of its period equal to 78.8 years. The same “80-year” cycle was found in auroral intensity since A.D. 400 by *Link* [1963]. In another analysis based on a record of auroral frequency numbers from A.D. 290 onwards, *Gleissberg* [1965] reported the period to be equal to 82 years.

[6] Moreover, some distinctive features of the shape of the Gleissberg cycle curve were established. For example, there is a well known Waldmeier’s rule for the 11-year cycle wave which establishes inverse dependence of the time of ascent on the intensity of its maximum [*Vitinskii et al.*, 1986]. Unlike that, the corresponding dependence for the Gleissberg cycle turned out to be direct: “the longer the period of ascent, the higher the ascent” [*Rubashev*, 1964; *Gleissberg*, 1966], the same direct proportional relation holds for the descent part of the wave, with mean lengths of ascent and descent equal to 38 and 41 years, respectively [*Gleissberg*, 1966].

[7] Another astronomical indicator of solar activity proposed and used in astronomical studies is related to statistical features of the behavior of the groups of sunspots. That index is the importance of sunspot groups [*Kopecký*, 1960, 1962] which represents statistical features of the groups of sunspots. Based on that *Kopecký* [1962, 1964] presented evidence of the reality of the “80-year” cycle and suggested a hypothesis of its physical mechanism. *Kopecký* [1976] inferred that the timing of the last (as of that time) maximum of the “80-year” cycle had happened at the cycle No.18 (1944–1953) not when the highest peak in sunspot numbers occurred during the cycle No.19 (1954–1964). That has essentially confirmed the assertion made by *Gleissberg* [1976] that a maximum of the “80-year” cycle occurred at around 1950. Finally, *Kopecký* [1991] deduced that the timing of the last minimum of the cycle had likely happened at cycle No.20 and that during cycles No.21 and 22 the Gleissberg cycle was already on the ascending phase.

[8] Furthermore, a variation with Gleissberg-like period was reported to be found even for the more “global” characteristics of the Sun—solar radius variations over the past 265 years [*Gilliland*, 1981]. A result of statistical analysis of a few data sets was claimed that the secular radius experiences a variation of an amplitude equal to $\pm\sim 0.2''$ (0.02%) with a period of 76 years with a maximum

at about A.D. 1911 and that it is negatively correlated with the Gleissberg cycle of mean sunspot numbers. In another work by *Sofia et al.* [1985] the historical record of the Sun’s diameter obtained from timings of eclipses was subject to harmonic analysis with one period equal to 90 years. The amplitude of that cycle was inferred to be little less than $\pm\sim 0.5''$. However, these results are not yet accepted because, understandably, such kind of assessment is difficult to infer with a high reliability from the measurements of solar radius which, according to *Emilio et al.* [2000], are “neither consistent nor conclusive”.

[9] At the same time the reality of a secular periodic variation in solar and solar–terrestrial phenomena has been argued (see reviews by *Kopecký* [1964], *Siscoe* [1980], and *Feynman and Fougere* [1984]). First of all, the period of the cycle in question was uncertain. In different studies the length of the period of the secular variation was determined to be equal to 95 years, 65 years, 55 years, 58 years, 83 years, 78.8 years, 87 years [*Siscoe*, 1980; *Feynman and Fougere*, 1984]. That situation is understandable, because the longest record of direct observations of solar activity was and still is the sunspot numbers which provides more or less reliable information since 1700 (see below). That gives one only 300 years of time span by now which encompasses ≈ 3.4 periods of Gleissberg cycle which is quite low for its statistical analysis. And at the time of earlier studies that record was even shorter so they failed to reveal the longer cycles than 11 years by objective quantitative methods like methods of spectral analysis (see account by *Gleissberg* [1958]). With onset of the methods of spectral analysis more efficiently coping with length of the record not sufficiently longer (say, 3–5 times) than the period in question, like Burg’s maximum entropy method (MEM), it has become a feasible task. For example, *Wittmann* [1978] performed MEM spectral analysis on sunspot number data for 1700–1976 (277 years) which revealed a long cycle of 92.42 years period.

[10] Still much of the evidence for existence of the cycle was established on the basis of auroral records [*Gleissberg*, 1958; *Link*, 1963; *Gleissberg*, 1965; *Siscoe*, 1980; *Feynman*, 1983; *Feynman and Fougere*, 1984]. The most decisive evidence for the Gleissberg periodicity in solar–terrestrial phenomena was brought by a maximum entropy spectral analysis of the number of aurora reported per decade in Europe and the Orient from 450 A.D. to 1450 A.D. [*Feynman and Fougere*, 1984]. It revealed a strong and stable line at 88.4 ± 0.7 years for the time span of the last ~ 11 Gleissberg cycles which cover an interval of almost 1000 years. Another confirmation of 88-year cycle was presented by *Attolini et al.* [1988, 1990] from spectral analysis by Blackman-Tukey (correlation-spectral) method of decennial frequency of aurora record over the 689 B.C.–1519 A.D. compiled by *Attolini et al.* [1988].

[11] The dynamics of variations in long records of cosmogenic isotope ^{14}C has been already studied very intensively via correlogram analysis [*Lin et al.*, 1975; *Sonett*, 1984] and via various methods of Fourier spectral analysis [*Sonett*, 1984; *Attolini et al.*, 1987; *Sonett and Finney*, 1990; *Damon and Sonnett*, 1991; *Cini Castagnoli et al.*, 1992]. As a result, a number of components of conspicuous cyclic nature were reported. We can mention among them a dominant quasiperiodicity of 2200–2400 years [*Suess*, 1980; *Sonett and Finney*, 1990; *Damon and Sonett*, 1991]

named *Hallstattzeit* cycle by *Damon and Sonett* [1991] due to an obvious link to a sequence of strong climatic events in late Earth's climatic history. Another example of a strong periodic component of $\sim 208\text{--}212$ years period (Suess cycle) was found in a number of time records of cosmogenic ^{14}C [*Suess*, 1980; *Sonett*, 1984; *Damon and Sonett*, 1991; *Stuiver and Braziunas*, 1993].

[12] *Lin et al.* [1975] analyzed a compiled time series of ^{14}C content in tree rings by carrying out correlogram analysis. By comparison with the correlogram of sunspot numbers which exhibited some periodicity ca. 100–110 years, the correlogram of detrended radiocarbon time series definitely indicated a periodicity about 80 years and another one at ca. 350 years. *Feynman* [1983] considered two ^{14}C records and drew attention to the fact that the analysis of the whole-range 8000-year record by *Lin et al.* [1975] provides a good indication of the periodicity in the region of 80 years whereas another analysis of the post-700 A.D. rates of ^{14}C production did not indicate any spectral power increase in the 60–100-year period range. In another work on spectral analysis of long radiocarbon and other terrestrial records *Cini Castagnoli et al.* [1992] gave special attention to manifestation of the Gleissberg periodicity in Fourier spectra. The periodogram and maximum entropy methods (with autoregressive order $AR = 150$) were used which both indicated presence of a Gleissberg-like peak in the spectra: 88 and 86–87 years, respectively. *Raisbeck et al.* [1990] obtained a time record of another cosmogenic isotope variations from Antarctica comprising the data on concentration of ^{10}Be in ice core acquired at the polar station *South Pole* and extending over the past ca. 1100 years. The spectral analysis of those variations revealed two equally high dominant peaks with periods of 93 years and 202 years.

[13] Another direction for studies of solar activity in the past is measurement of the concentration of cosmogenic isotopes in meteorites [*Honda and Arnold*, 1964; *Vogt et al.*, 1990; *Michel et al.*, 1991]. One of the isotopes used to study cosmic ray variations is ^{44}Ti which is produced in space in meteoritic iron and nickel [*Bonino*, 1993]. Intensified studies of proxies of the secular variations of galactic cosmic rays (GCR) during the last two centuries are carried out by measurements of ^{44}Ti in stony meteorites (chondrites) [*Bonino et al.*, 1994, 1995a, 1995b, 1997, 1998]. ^{44}Ti has a much shorter half-life than such cosmogenic isotopes as ^{14}C (5730 years) and ^{10}Be ($1.5 \cdot 10^6$ years). Its half-life has been recently adjusted to $T_{1/2} = 59.2 \pm 0.6$ years (1σ error level) as a weighted average of combined results measured in three laboratories [*Ahmad et al.*, 1998]. Therefore it is more effective in studies of cosmic rays in the past for the time span of one or two centuries. It is produced in GCR interactions (>70 MeV) in meteoritic Fe and Ni at the estimated rate ~ 1 atom/min per kg meteorite [*Honda and Arnold*, 1964]. To determine the production rate, it is necessary to correct the measured activity for variation in target element (Fe, Ni) concentration and for shielding depth within the meteoroid, and to calculate the activity at the time of fall [*Bonino et al.*, 1998].

[14] *Bonino et al.* [1995a] had measured the activity of nine chondrites fallen on the Earth within the time period A.D. 1883–1992. Originally they used for calculations the half-life of ^{44}Ti which at that time was known to be $T_{1/2} = 66.6$ years. That study was further developed by *Bonino et*

al. [1998] in extending the time span of coverage by 13 meteorite specimen to 1840–1996 with the newly accepted value of the ^{44}Ti half-life. Their updated result presents a time profile of ^{44}Ti abundance in chondrites with one maximum indicated by meteorites Cereseto (1840) and Grüneberg (1841) and with another broad maximum indicated by meteorites Rio Negro (1934) and Monze (1950). These maxima occur with a time lag of 30–40 years after assumed maxima in GCR intensity (corresponding to prolonged minima in envelope of the Schwabe cycle at the Dalton Minimum around 1800 and around 1910 at one of the minima of the Gleissberg cycle). That time lag is anticipated as the result of the process of generation and decay of ^{44}Ti in meteorites during their exposure to GCR in space. There is a continuing puzzle in the magnitude of increase (20–30%) of ^{44}Ti abundance [*Bonino et al.*, 1997, 1998] at the extrema which is 3–4 times higher than expected from theoretical predictions [*Bhandari et al.*, 1989]. That issue was specifically addressed by *Neumann et al.* [1997] where the new and more accurate ^{44}Ti production rates for more realistic irradiation conditions were calculated based on new measurements of cross-sections in radiation experiments. A new theoretical prediction of the ^{44}Ti abundance in meteorites, based on a recent calculation of the solar modulation of the galactic cosmic ray spectra in the past, and taking also into account the new cross-sections, gives a good agreement with the experimental values [*Bonino et al.*, 2001, 2002].

[15] Another direction of paleoastrophysical studies of the solar activity in the past is the measurement of thermoluminescence (TL) in the layers of stratified columns of sea sediments. The analysis of the TL profile of sea sedimentary cores by *Cini Castagnoli et al.* [1988] pointed to the existence of long-term cycle with a period of 82.6 years. *Cini Castagnoli et al.* [1989] found significant peaks with the following periods: 12.06 and 10.8 years, along with 59 and 137.7 years. According to *Cini Castagnoli et al.* [1989] such realization may be a result of amplitude modulation by 206-year cycle applied to cycles with periods of 11.4 and 82.6 years. Another analysis of the total carbonate and TL profiles of an Ionian sea sediment core by *Cini Castagnoli et al.* [1994] revealed, even at two different sampling of the core layers, the Gleissberg cycle at 83 and 92 years.

[16] *Attolini et al.* [1987, 1988] were the first to study the time behavior of the Gleissberg cycle and another, 130 years, periodicity in long time series of the cosmogenic isotopes ^{14}C and ^{10}Be . Along with the conventional periodogram technique of Fourier spectral analysis they used another technique that they developed, cyclogram analysis, which allows tracking the behavior of a selected harmonic component in time [*Attolini et al.*, 1984]. Another technique they usually used was the method of folding epochs. Both techniques confirmed the persistence of the 86-year period from 4400 B.C. through 2530 B.C. in long time series of ^{14}C [*Attolini et al.*, 1988]. They also noticed that the 88-year cycle was not uniformly present in solar–terrestrial data. As interpretation they proposed that the 88-year cycle might be a subharmonics of the 11-year Schwabe cycle which acts as a fundamental [*Attolini et al.*, 1987].

[17] Possible physical mechanisms of the Gleissberg cycle as an 80-year period of the average importance of sunspot groups were discussed by *Kopecký* [1962]. The

origin of the Gleissberg cycle in terms of modern theory of astrophysical dynamo models was intensively studied by Tobias [1996, 1997]. In a recent work Pipin [1999] considered the Gleissberg cycle to be the result of the magnetic influence upon angular momentum fluxes driving the differential rotation in the shell of the solar convection zone.

[18] All the above reviewed studies were concerned with: 1) the manifestation and features of time behavior of the Gleissberg cycle during the last ~ 300 -year period of direct and detailed observations of sunspot activity; 2) demonstration of the existence of the Gleissberg cycle in other solar–terrestrial records such as epochs of maxima of aurora sightings going back for ~ 2000 years despite the imperfect record; 3) studies of cosmogenic isotopes in meteorites extending back to the Maunder Minimum; 4) the use of the existing data on cosmogenic isotopes extending back over the range of a few thousand years. In this work we take advantage of the existence of an improved cosmogenic isotope record that was extended back to 12,000 years before present (B.P.). Availability of these data provides us an opportunity to explore the continuity, stability and possible intermittency of the Gleissberg cycle over a longer timescale and apply more advanced methods and procedures of time series analysis. Those methods allow us to track back in time the behavior of the whole process rather than just one selected frequency as cyclogram analysis does. In this work we confine the scope of our study to manifestations of the Gleissberg cycle in some solar–terrestrial phenomena. We make emphasis on its duration, on determination of some quantitative characteristics of the cycle, and on examination of permanence and uniformity of its manifestation.

2. Gleissberg Cycle in Direct Astronomical Data

[19] As mentioned above, both the amplitude and the period of the “11-year” Schwabe cycle of Wolf sunspot numbers experience quite significant variations as depicted in Figure 1. Annually updated sunspot data are provided by World Data Center A for Solar–Terrestrial Physics [McKinnon, 1987] with the record starting at A.D. 1700. That time interval encompasses the final part of the long time period from 1645 through 1705, called Maunder Minimum by Eddy [1976], when the Sun remained in an extremely quiet state with sunspot activity strongly suppressed.

[20] “Secular smoothing” procedure was introduced by Gleissberg [1944, 1958] as a 5-point symmetric trapezoidal lowpass filter [Gleissberg, 1958]:

$$\tilde{\mathcal{H}}_{\text{Sec}}\{\tilde{y}\}[i] = \frac{1}{8} \cdot \left[y(t_{i-2}) + 2 \cdot \sum_{k=-1}^1 y(t_{i+k}) + y(t_{i+2}) \right] \quad (1)$$

The filter shows good selectivity: it effectively suppresses the amplitudes of the variations faster than ca. 50 years by at least 10 times or more. At the same time it preserves the phase of oscillations for all periods higher than 44 years.

[21] Applying the Gleissberg’s “secular smoothing” to both heights of maxima and separately to dates of minima and maxima of sunspot number records then merging them, one obtains a variation of both amplitude—amplitude modulation (AM) and period—frequency modulation (FM) of the Schwabe sunspot cycle. The reviews of quite exhaustively

studied amplitude modulation can be found in monographs by Vitinskii [1965] and Vitinskii *et al.* [1986]. The frequency modulation was also intensively studied in a number of publications, for example, by Dewey [1958], Vasili’ev [1970], Attolini *et al.* [1985], Mordinov [1988], and also by one of the authors of this paper [Peristykh, 1990; Kocharov and Peristykh, 1990, 1991; Peristykh, 1993, 1995].

[22] The variations of the height of the 11-year cycle (SCH) of sunspot numbers are depicted in Figure 2a and indicate a prominent periodicity shorter than 100 years. There is a well-expressed long-term trend showing that the magnitude of solar activity is steadfastly increasing in 20th century. The detrended residual time series exhibits obvious oscillatory behavior.

[23] It was processed by harmonic analysis which is basically a procedure consisting of trigonometric regression on a set of m basic angular frequencies $\vec{\omega}_b$ [Dmitriev *et al.*, 1987] detected first by methods of spectral analysis which can be mathematically formulated as a two-stage procedure:

$$\vec{\alpha}_{LS}(\vec{t}_s, \vec{y}_{obs}, \vec{\omega}_b) = \arg \min_{\vec{\alpha} \in \mathbb{R}^{2m+1}} \{ \|\vec{y}_{obs} - \hat{\Phi}^\top(\vec{\omega}_b, \vec{t}_s)\vec{\alpha}\|^2 \} \quad (2a)$$

$$\vec{y}_{rec} = \hat{\Phi}^\top(\vec{\omega}_b, \vec{t}_s)\vec{\alpha}_{LS} \quad (2b)$$

Here the first stage is a statistical procedure of least squares (LS) estimation of the vector $\vec{\alpha}_{LS}$ of the parameters of $2m + 1$ trigonometric polynomials (one of them is a constant) approximating the vector \vec{y}_{obs} of given data series over the vector \vec{t}_s of N sampling time moments in LS sense. The matrix of functions $\hat{\Phi}(\vec{\omega}_b, \vec{t}_s)$ consists of the values of trigonometric polynomials at sampling time moments. The second stage is the construction of the polyharmonic regression \vec{y}_{rec} of the time series over the sampling time moments \vec{t}_s .

[24] A simple monoharmonic regression with fundamental period of 88 years yields a very good approximation of the smoothed curve. The secular smoothed curve displays three major maxima at 1778, 1860 and 1947 with increments of 82 and 87 years, and two indicative minima at 1816 and between 1893 and 1917 give us increment of 89 years, correspondingly. That matches very well with epochs of the monoharmonic fitted to the smoothed curve with maxima at 1771, 1860 and 1955, and with minima at 1724, 1816, 1902 and 1983. The maximum at 1947 is in accord with Kopecký [1976] who reported the last maximum of the “80-year” cycle within the time interval 1944–1953. At the same time the estimate of the last minimum of the “80-year” cycle within the Schwabe cycle No.20 by Kopecký [1991] which corresponds to the interval 1964–1976 is strongly biased. That bias is easily noticed in Figure 2a and can be explained by influence of the strong negative fluctuation in SCH after 1950.

[25] The changes of the period of the Schwabe cycle in relative sunspot numbers are presented as solar cycle length (SCL) variations in Figure 2b. There is a faint long-term trend showing that the SCL is slightly decreasing in 20th century. The curve smoothed by secular smoother indicates a conspicuous periodicity slightly shorter than 100 years with three well timed maxima (of inverted curve) at 1766, 1849 and 1933–1943, and three well expressed minima at 1717, 1798, 1890 and one not as distinct within the range

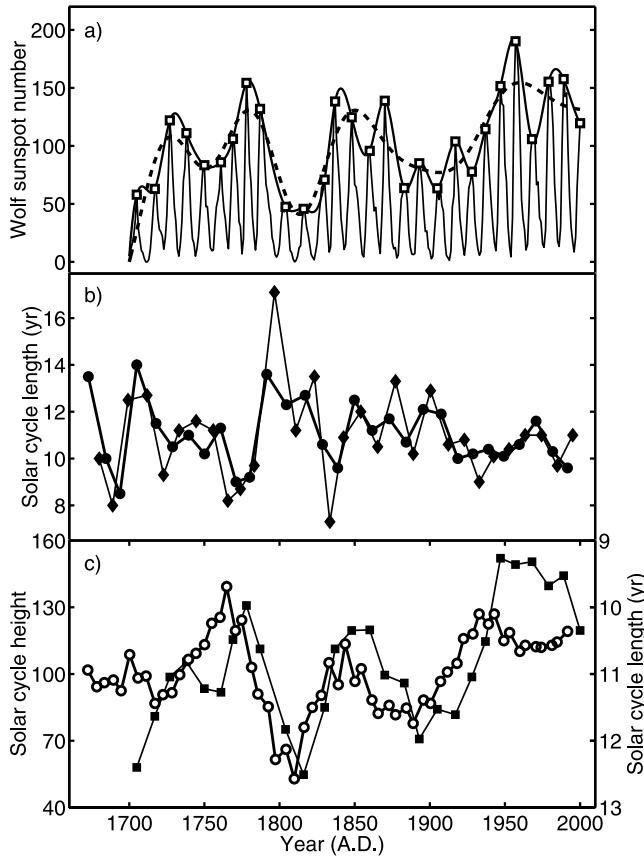


Figure 1. a) Variations of the height of the 11-year cycle of sunspot numbers: sunspot number curve (—); envelope of sunspot number curve (\square —); envelope smoothed by lowpass filter (- - -). b) Variations of the cycle length of the 11-year cycle of sunspot numbers: minimum to minimum (\bullet —); maximum to maximum (\blacklozenge —). c) Juxtaposed variations of the height (\blacksquare —) and cycle length (two data sets “min–min” and “max–max” from the panel (b) merged) (\circ —) of the 11-year cycle of sunspot numbers both filtered by “secular smoother” (see description in text).

1958–1986 with increments 83, 89 years, and 81, 92 and 76.5 years, respectively. That matches very well with epochs of the monoharmonic fitted to the smoothed curve with maxima at 1761, 1850 and 1939, and with minima at 1717, 1805, 1894 and 1983.

[26] Finally, we must note that the sunspot record is subject to certain limitations. First, the record of relative sunspot numbers is not homogeneous: the quality or statistical reliability of the data is not uniform and significantly declines for the earlier dates. As explained by *Eddy* [1977] and *McKinnon* [1987], the data from 1848 and on are “reliable”, for the time span 1818–1847 they are “good”, between 1749 and 1817 they are “fair”, and for the time interval 1700–1748 they are “poor”. Even though, among all available solar or solar–terrestrial direct observational data (except on auroral frequency but they are scarce) the sunspot number record is the longest while most of the others do not extend before the 1860s [*Eddy*, 1975]. It was possible to extend the record, though with a few time intervals containing lacunas during the Maunder Minimum, back to A.D. 1610 [*Eddy*, 1976]. All other solar observa-

tional records are much shorter than relative sunspot number and it is not easy to juxtapose them even for modern dates because of the relative inhomogeneity with respect to one another thoroughly discussed by *Kopecký et al.* [1980].

[27] These limitations do not in any extent undermine the importance of such kind of analysis of epochs of the minima and maxima of the Schwabe cycle initiated by W. Gleissberg. It sets ground for further analyses using other kinds of data, especially the records of cosmic radiation in the past as represented by the data on cosmogenic isotopes.

3. Cosmogenic Isotope Concentration in the Earth’s Atmosphere as an Effective Proxy Indicator of Solar Activity

[28] The most celebrated cosmogenic isotope is ^{14}C (coined by W.F. Libby as radiocarbon). It gained its great fame undoubtedly because of radiocarbon dating method [*Libby*, 1955]. Radiocarbon is generated in the atmosphere by the nuclear reaction $^{14}\text{N}(n, p)^{14}\text{C}$. Fast neutrons are produced in spallation reactions on atmospheric gases during nuclear cascade processes initiated primarily by galactic cosmic rays [*Lal and Peters*, 1967]. About 65% of the fast

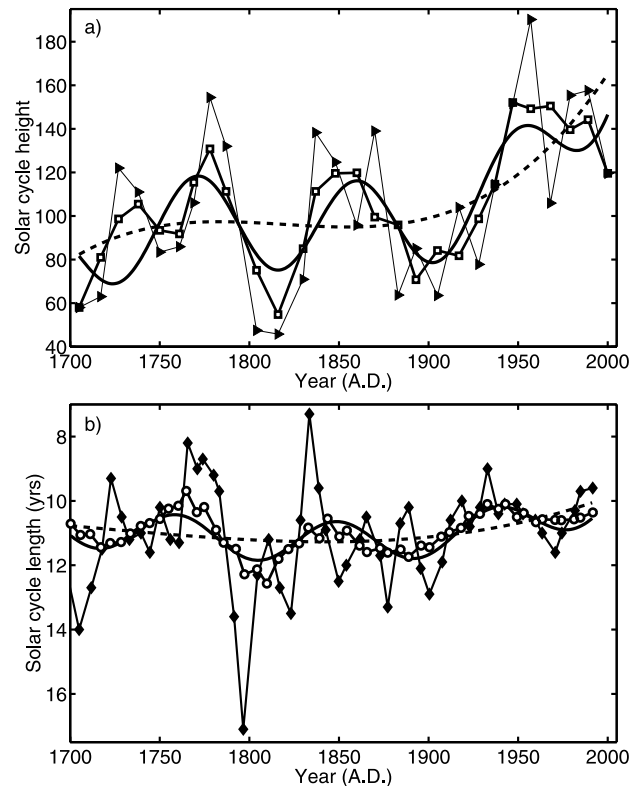


Figure 2. a) Variations of the height of the 11-year sunspot cycle: raw (\blacktriangleright —); lowpass filtered by secular smoothing $\mathcal{H}_{Sec}\{\cdot\}$ (\square —); long-term cubic trend (- - -); and trigonometric monoharmonic ($T_{bas} = 88$ years) regression combined with the trend (—). b) Variations of the length of the 11-year sunspot cycle (two data sets “min–min” and “max–max” from the Figure 1b merged): raw (\blacklozenge —); lowpass filtered by secular smoothing $\mathcal{H}_{Sec}\{\cdot\}$ (\circ —); long-term parabolic trend (- - -); and trigonometric monoharmonic ($T_{bas} = 88$ years) regression combined with the trend (—).

neutrons are thermalized, producing ^{14}C . The intensity of GCR entering the Earth's atmosphere depends on the state of solar activity via the magnetic field imbedded in the solar wind. As solar activity increases, fewer GCR enter the atmosphere to produce ^{14}C . Consequently, there is an inverse relationship between ^{14}C production and solar activity first found by *Stuiver* [1961, 1965].

[29] Radiocarbon rapidly equilibrates with atmospheric CO_2 and enters the biogeochemical cycle of carbon including the life cycle of plants and animals. After the organism dies or a part ceases to participate in the C–O cycle, $^{14}\text{CO}_2$ is no longer replaced and radiocarbon decays as follows $^{14}\text{C} \rightarrow ^{14}\text{N}^+ + \beta^- + \nu$ with half-life of 5730 years. Atmospheric CO_2 assimilated by trees is the only source of carbon contributing to the growth of the annual tree rings that are formed every year during the growing season. Thus, the annual rings of trees are natural archives conserving the record of past ^{14}C concentration in the atmosphere.

[30] The abundance of ^{14}C in samples is obtained either indirectly via measurements of specific radioactivity of carbon material by liquid scintillation or proportional gas counting of ^{14}C β -decay or directly by atom counting via accelerator mass spectrometry. The results of β -counting are expressed in terms of specific activity of the sample measured $A_s = -\lambda N$ where λ is radioactive decay constant and N is number of atoms of the isotope per 1 g of sample. In geophysical studies, we are interested in the activity of ^{14}C in the past relative to the normalized and isotopic fractionation corrected standard A_{on} . In this calculation, the precise half-life $T_{1/2} = 5,730$ years is used and a quantity $\Delta^{14}\text{C}$ is obtained as follows:

$$\Delta^{14}\text{C} = [A_{sn}/A_{on} \cdot e^{\lambda\tau_s} - 1] \cdot 1000, \text{‰} \quad (3)$$

where τ_s is the age of the sample prior to A.D. 1950. The activity of the samples are also corrected for isotopic fractionation. $\Delta^{14}\text{C}$ represents concentration of ^{14}C in the atmosphere at any time in the past relative to an international standard that is normalized such that $\Delta^{14}\text{C}$ passes through zero at mid-19th century prior to the large increase of CO_2 due to combustion of fossil fuels. For example, at the University of Arizona ^{14}C is measured by state-of-the-art scintillation counting (*Quantulus*) in an underground laboratory with a precision equal to or less than 0.2% or by accelerator mass spectrometry (AMS) with a precision of 0.3% (when using 4 targets).

[31] Originally the radiocarbon dating method was based on the assumption that the specific activity of atmospheric ^{14}C was temporally and geographically constant which also implies constant intensity of cosmic rays producing cosmogenic isotopes. However, quite soon it was found from inconsistencies of the dates obtained by radiocarbon dating that intensity undergoes quite significant temporal variations [de Vries, 1958; see also Suess, 1970; Stuiver and Quay, 1980; Damon et al., 1978]. The physical relationship between $\Delta^{14}\text{C}_{atm}$ and intensity of CR can be represented as a convolution integral:

$$\Delta^{14}\text{C}(t) = \int_{-\infty}^t h_A(t - \tau, T_C(t - \tau)) Q(\tau, W(\tau), M(\tau)) d\tau \quad (4)$$

where $h_A(t)$ is a kernel time function of system response of the Earth's distributive system of carbon; $Q(t, W(t), M(t))$ is a time function of the ^{14}C production rate by incident cosmic rays in the Earth's atmosphere which in turn depends on time functions of the level of solar activity $W(t)$ and intensity of the geomagnetic field $M(t)$ (its dipole component); $T_C(t)$ is a time function indicating the climate of the Earth which could influence the processes of redistribution of the cosmogenic isotope in the biogeochemical cycle. The dependence of the production rate Q as a function of geomagnetic dipole moment is well known [Elsasser et al., 1956]: $Q(t, M(t))/Q_0 = (M(t)/M_0)^{-0.52}$ and sufficient archeomagnetic data are available for the last 10,000 years [Merrill et al., 1996] to make allowance for that effect and also to show that the dipole moment is the dominant factor causing the long-term trend of $\Delta^{14}\text{C}_{atm}$. Regarding the climatic influence, fortunately the Earth's climate during the Holocene (last 11,700) has been surprisingly stable and constitutes a minor factor in $\Delta^{14}\text{C}_{atm}$ variations during the time of interest of this paper.

[32] The necessity for correction of the method led to large-scale measurements of the ^{14}C concentration in various terrestrial samples dated by other, independent methods. Mostly, those samples were represented by annual growth tree rings which can be reliably dated back by ring counting and patterns matching procedures. As a result of long-lasting research efforts, a few long time records of ^{14}C concentration in atmosphere of the Earth were obtained. The longest almost continuous, unbroken time series of cosmogenic isotope abundance in terrestrial dated samples is represented by calibration record INTCAL98 comprising predominantly decadal data on $\Delta^{14}\text{C}$ in annual tree rings and coral rings [Stuiver et al., 1998]. The $\Delta^{14}\text{C}$ data back to ~ 9900 B.C. were obtained on measurements of dendrochronologically dated tree rings by state-of-the-art beta-counting at precision of ca. $\pm(0.2-0.3)\text{‰}$ depending on the age of the sample. Prior to ~ 9900 B.C. the analyses were obtained by accelerator mass spectrometry (AMS) and the reference age by radiometric measurement of ^{230}Th in small samples of corals at precision $\geq 10\text{‰}$ for $\Delta^{14}\text{C}$.

[33] The time variation of cosmogenic ^{14}C concentration in the Earth's atmosphere $\Delta^{14}\text{C}_{atm}$ in the past is depicted in Figure 3a as provided by that record. The time series exhibits a large-scale long-term trend due to primarily changes in the intensity of the dipole moment of the geomagnetic field. To emphasize the long-term trend an adaptive lowpass filtering by smoothing splines was applied giving us the component with slow rate of change (Figure 3a).

[34] This method, in contrast to an interpolating cubic spline, approximates the observational data $\{y_i, i = 1, \dots, n\}$ with rescaling weights δy_i trading that for higher smoothness through minimizing the following functional:

$$\sum_{i=1}^n \left[\frac{f(x_i) - y_i}{\delta y_i} \right]^2 + S \cdot \int_{x_1}^{x_n} [f''(x)]^2 dx \quad (5)$$

where S is some given (specifically chosen) parameter specifying scaling. An advantage of the smoothing spline as a digital filter is monotony of its magnitude frequency response which means it does not have ripples and, therefore, it produces no artificial peaks in Fourier spectrum. Moreover, its magnitude frequency response

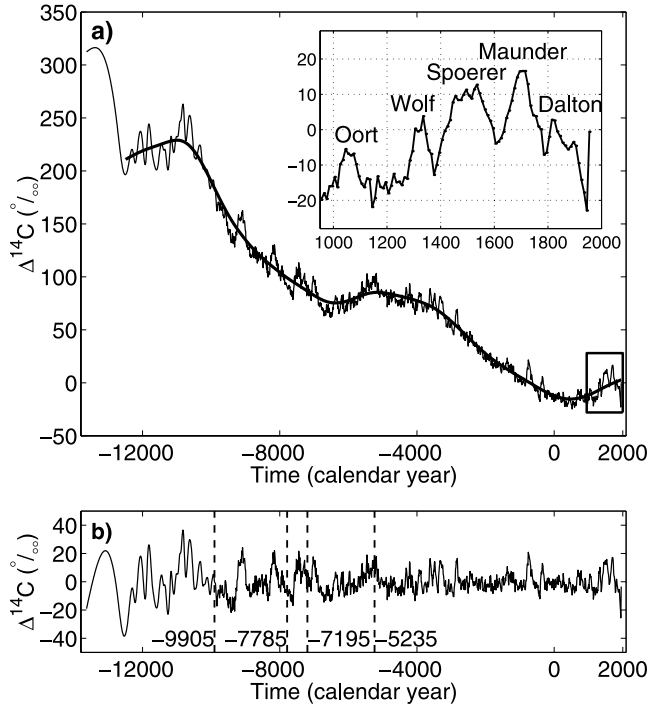


Figure 3. Time variations of cosmogenic ^{14}C concentration in the Earth's atmosphere ($\Delta^{14}\text{C}$) in the past (INTCAL98 record): a) raw (thin line) $\Delta^{14}\text{C}_{\text{atm}}(t)$ data (inset—the last millennium of the record) and long-term trend (thick line) obtained by applying smoothing spline $\mathcal{H}_{\text{Spl}}(8 \cdot 10^3, 0.99) \{ \Delta^{14}\text{C}_{\text{atm}} \}$, b) the raw data with the trend subtracted. Note in the inset the sharp decrease in $\Delta^{14}\text{C}$ as a result of combustion of fossil fuels followed by sharp increase due to beginning of nuclear explosions.

function can be expressed by a simple formula with only one given parameter (determining rigidity of the spline) which, being changed, defines a bundle of similar curves intersecting only at zero frequency. Hence, it is uniquely defined by specifying its any single point (except, of course, zero frequency). Therefore, one totally determines all properties of the gain of a smoothing-spline filter $\mathcal{H}_{\text{Spl}}(T, G_T) \{ \cdot \}$ by specifying the value of its gain G_T at some chosen value of period T years of interest. Another advantage of this technique is its zero phase shift which means it does not distort the shape of the signal.

[35] After the trend obtained by smoothing spline filtering with the parameters $T = 8000$ years and $G_T = 0.99$ is subtracted from the original data, one obtains a residual time series of deviations from the general trend (Figure 3b):

$$\Delta^{14}\text{C}_{\text{atm}}^{\text{detr}}(t) = \Delta^{14}\text{C}_{\text{atm}}(t) - \mathcal{H}_{\text{Spl}}(8 \cdot 10^3, 0.99) \{ \Delta^{14}\text{C}_{\text{atm}}(t) \} \quad (6)$$

consisting of high-frequency variational components, that is equivalent to applying highpass filtering.

4. Gleissberg Cycle in Cosmogenic Isotope Variations

[36] We conducted study of the dynamics of variations in the $\Delta^{14}\text{C}$ time series of INTAL98 record. First, conven-

tional spectral analysis was performed. We favored the Discrete Fourier Transform (DFT) as a good nonparametric, robust yet clearly transparent, method for pilot analyses. Rather than plotting the spectral power of the signal we preferred to plot its square root (denoted here as “DFT amplitude”) which as a very good approximation can give one a good perception of the distribution of the magnitude of various processes. This is especially useful for comparison of the contribution of various periodic components by the height of their corresponding peaks. The strong long-term trend in data discussed above would produce low-frequency components of overwhelming power in spectrum which would have serious impact on spectral peaks in adjacent range of the spectrum. To combat that effect the output of the above mentioned lowpass filtering via smoothing splines is subtracted from the raw data according to (6) and the resultant time series $\Delta^{14}\text{C}_{\text{atm}}^{\text{detr}}$ is subject to spectral analysis [Damon and Peristykh, 2000].

[37] The whole Fourier spectrum of $\Delta^{14}\text{C}_{\text{atm}}^{\text{detr}}$ is depicted in Figure 4. First look reveals, that the spectrum displays all so far known features as the predominant peak at ca. 2300 years, conspicuous 208-year peak of Suess cycle, also its second harmonic (first overtone) of 104-year period. It indicates well pronounced and highly resolved peak corresponding to ca. 88-year cycle, in which we have special interest, with the peak at 44.9-year period correspondent to its second harmonic, also well resolved. Besides that, additional peaks of ca. 150 years and ca. 61 years are present in the spectrum.

[38] Another problem that had to be taken into consideration was the homogeneity of the INTAL98 record [Damon and Peristykh, 2000]. There were some additional corrections in dendrochronological age of samples. Prior to 5242 B.C. ages were increased by 41 years and prior to 7792 B.C. ages were increased by 95 years. Prior to 7195 B.C. there are some gaps in the $\Delta^{14}\text{C}$ record (specifically at 9835, 9675, 9155, 9045, 9025, 8815, 8775, 7985, 7775,

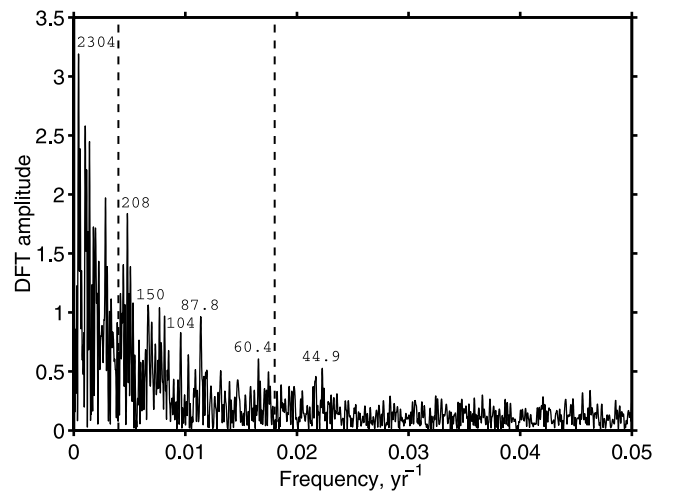


Figure 4. Fourier spectrum (DFT, Dirichlet window) of detrended $\Delta^{14}\text{C}$ variations in the INTAL98 record for the whole frequency range. Dashed lines mark the frequency range of special interest which is plotted in more details in Figure 5.

7355, 7275 and 7195 B.C.) but this aspect of inhomogeneity was not of primary concern because gapped time intervals can be and usually are routinely interpolated without causing a problem for data processing. Taking all that into account three consecutively increasing time intervals were chosen for spectral analysis of detrended data from Figure 3b: 5242 B.C.–1895 A.D., 7792 B.C.–1895 A.D. and 9905 B.C.–1895 A.D. (whole tree ring based time interval).

[39] Two variants of the periodogram method of spectral analysis were used to obtain those spectra. The first one is plain DFT method and the second one is Welch's modified windowed periodogram method of spectral analysis [Giordano and Hsu, 1985] which allows us to decrease the variance of the PSD estimate as a statistical variable. In order to equalize treatment of the most of data samples, a symmetric 50% overlap of Tukey-Hamming time window [Cadzow, 1987] was used. For L -long segments ($L = [N/M]$ where N is the whole time series length, and M was set to 2 and 3) that provides us with $2 \cdot M - 1$ segments.

[40] The Fourier spectra of radiocarbon variations at above mentioned record breaks are depicted in Figure 5. As one can see, all three spectra display very stable features despite of all combinations of changing spectral resolution due to extending the time span covered by time series (7137, 9687 and 11,800 years, correspondingly) and subdividing the whole record into subintervals. They are the following.

[41] There is a prominent peak corresponding to the 88-year Gleissberg cycle ($f_1^G = 1/88 \text{ yr}^{-1} \approx 0.0114 \text{ yr}^{-1}$) along with its counterpart—peak corresponding to the 208-year Suess cycle ($f_1^S = 1/208 \text{ yr}^{-1} \approx 0.00481 \text{ yr}^{-1}$) along with a quite prominent 104-year peak obviously due to the second harmonic of the Suess cycle.

[42] One can also notice peaks of combination (“beat”) tones due to amplitude modulation of the 88-year cycle by the 208-year cycle: $f_1^{G \times S} = f_1^G \pm f_1^S$, so the corresponding periods are:

$$T_{1-}^{G \times S} = (f_1^G - f_1^S)^{-1} \approx 152 \text{ years}$$

and

$$T_{1+}^{G \times S} = (f_1^G + f_1^S)^{-1} \approx 61.8 \text{ years.}$$

Furthermore, one can notice more closely located and less pronounced sidebands of 88-year peak as manifestation of its AM by a cyclic component with frequency of *Hallstattzeit* cycle $f_1^H = 1/2200 \text{ yr}^{-1} \approx 0.00045 \text{ yr}^{-1}$: $f_1^{G \times H} = f_1^G \pm f_1^H$ so we have corresponding periods of the peaks:

$$T_{1-}^{G \times H} = (f_1^G - f_1^H)^{-1} \approx 91.7 \text{ years}$$

and

$$T_{1+}^{G \times H} = (f_1^G + f_1^H)^{-1} \approx 84.6 \text{ years.}$$

[43] The next applied procedure of signal analysis was bandpass digital filtering of studied signal $\Delta^{14}\text{C}_{\text{atm}}^{\text{detrit}}(t)$. That

allows tracking selected cyclicities in narrower range of periods. First, the frequency range of the filter passband is to be chosen. As our primary interest in current work was Gleissberg (88-year) cycle, all bands were centered around frequency value $f_G = 0.01136 \text{ yr}^{-1}$.

[44] Two types of bandpass (BP) digital filters (DF) were used: finite impulse response (FIR) filter and infinite impulse response (IIR) filter. The choice of the filter design techniques was stipulated by fitness of their properties to the features of the signal intended to be preserved. The most desired feature of DF is high selectivity manifested by a very short transition region between the passband and the stopband which is mostly best implemented by the IIR filters. At the same time the FIR filters can readily meet linear phase specification to preserve the shape of the signal which a causal IIR filter cannot achieve. Eventually, two different types of DF provided us necessary versatility in retaining desired properties of the signal.

[45] First, a linear-phase FIR bandpass filter was constructed by constrained least squares (CLS) design (Figure 6a). We posed much stronger error restrictions on the low-frequency stopband than on the high-frequency stopband (Figure 6a) because of much higher spectral power of signal in the former we need to cope with. As a result the gain characteristics has bell-like shape and the curve between its two first nodes (zeros) is confined within a passband $f_p = [0.0102, 0.0123] \text{ yr}^{-1}$ ($T_p = [81.5, 98.3] \text{ yr}$). That passband essentially covers the whole range of the Gleissberg cycle's peak with its sidebands due to modulation. The filtered signal in time domain is depicted in Figure 7a. As one can notice the envelope of quasi-harmonic output process has well formed enhancement within time interval 6500–1000 B.C. and two intervals of amplitude suppression around 7000 and 500 B.C.

[46] The IIR type of bandpass filter is an elliptic Cauer filter which the most important property is that they can minimize the width of the transition region. Its passband encompasses $f_p = [0.0109, 0.0119] \text{ yr}^{-1}$ ($T_p = [84.2, 92.0] \text{ years}$) (Figure 6b). Its passband practically covers exclusively the range of the Gleissberg cycle's peak and its sidebands with uniform attenuation within the whole band. The resultant filtered signal in time domain is depicted in Figure 7b.

[47] As can be seen from Figure 6, the spectral power of two bandpass filtered signals is concentrated in three frequency bands: the band of central peak and two sidebands. The latter are in no way compact but are rather bundles of peaks themselves. Nevertheless, it is possible to ascribe some center-of-gravity value of the frequency to each sideband which is very close to the position of the highest peak in the bundle. Hence, one can apply harmonic analysis to these bandpass filtered signals. As discussed above, harmonic analysis (see equations (2a) and (2b)) as a trigonometric regression requires setting a set of basic periods detected by spectral analysis. Therefore, the first set of basic periods obtained from the spectrum (Figure 5c) of the longest time interval was $\{87.7, 91.7, 84.7\}$ years producing a triharmonic time variation (Figure 7c). Another set of basic periods was obtained from the average of the three conventional DFT spectra (Figures 5a–5c): $\{87.9, 91.6, 84.7\}$ years which triharmonic time variation is depicted in Figure 7d. It should be kept in mind that for

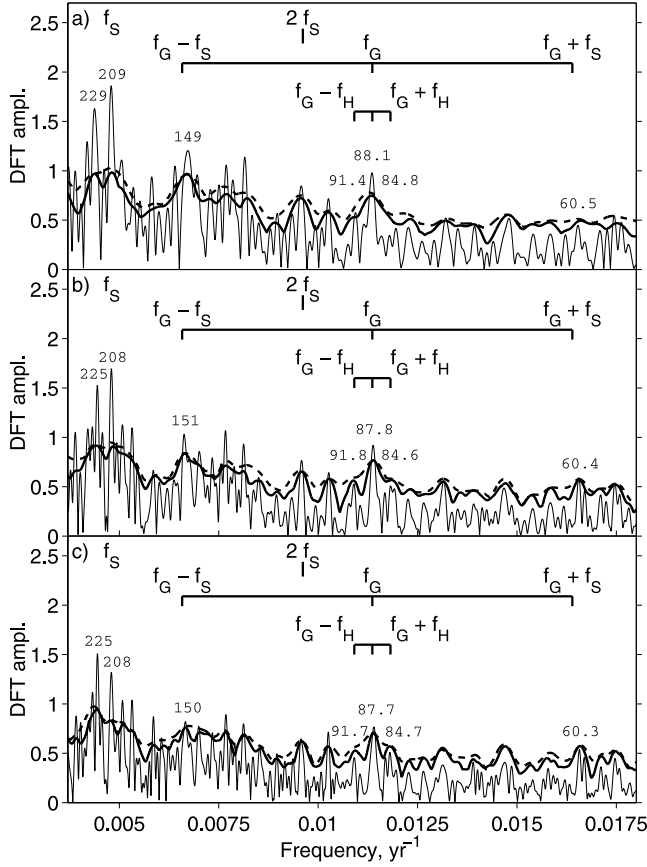


Figure 5. Fourier spectra of $\Delta^{14}\text{C}$ variations in the INTCAL98 record of decadal data for a) 5242 B.C.-1895 A.D., b) 7792 B.C.-1895 A.D., c) 9905 B.C.-1895 A.D.: plain DFT (thin line) and modified periodogram for $N/2$ - (thick line) and $N/3$ -long (dashed line) segments with 50% overlapping.

bandpass digital filtering implemented in Figures 7a–7b the nature of the signal processing inevitably produces end effects. One of the advantages of harmonic reconstruction is that it is free of end effects. In Figures 7c–7d we can observe a very close to ideal manifestation of beating phenomena which we cannot observe in Figures 7a–7b because of the larger number of spectral components within their passbands.

[48] A question could arise whether those variations of envelopes might be partially or totally a result of geomagnetic or climatic modulation. If that would be the case one could expect that such a variation would be manifested somewhat at all frequencies yielding together, according to Parseval's theorem, a variation in total variance. Having in mind a goal of tracking such effect we applied a technique of moving variance to detrended variations $\Delta^{14}\text{C}_{\text{atm}}^{\text{detr}}(t)$. Moving variance with window width $L_{\text{var}} = 510$ years (51 data points) versus position of the center of the window is depicted for comparison in all panels of Figure 7 (dashed line). The correlation coefficients of the moving variance with envelopes of the FIR filter and of the IIR filter were $r_{\text{FIR}} \approx -0.17$ and $r_{\text{IIR}} \approx -0.18$, correspondingly. This shows that the magnitude-scale variations of 88-year-cen-

tered narrow-passband processes extracted in different ways from $\Delta^{14}\text{C}_{\text{atm}}$ variations are essentially uncorrelated with each other. Hence, that strongly supports the idea of the independence of the Gleissberg-cycle amplitude variations from possible terrestrial influence on $\Delta^{14}\text{C}_{\text{atm}}$ variations.

5. Time–Frequency Analysis of Gleissberg Cycle in Cosmogenic Isotope Variations

[49] Spectral analysis does not tell us about how the characteristics of the signal change in time. That question should be addressed to Time–Frequency Analysis (TFA). In this work we follow the technique of Moving Periodogram Method (MPM) of TFA elaborated by *Peristyk* [1990] [see also *Kocharov and Peristyk*, 1990, 1991].

[50] The concept of it is very simple and can be expressed as follows. The Fourier Transform (FT) $\tilde{\mathcal{F}}_f\{\cdot\}$ is performed not upon the whole available record of the total time interval but rather upon a subinterval of fixed length while position of its center t' is moving from the beginning of the record toward its end. It is equivalent to a finite and rather short (compared to the total record length) time window (or data window) of weights $h(\tau)$ applied to the record. That is why it is otherwise called Short-Time Fourier Transform (STFT) which we will denote as $\tilde{S}_{t',f}^{h,\tau_w}\{\cdot\}$. The MPM variant of the TFA includes additional procedure of statistical noise estimation at every position of the moving window. In this work we did not actually need to perform that estimation because our scope was tracking in time a single chosen peak of the Gleissberg cycle which is conspicuous. As noted above for conventional spectral analysis, here we rather use the amplitude scale of Fourier spectrum than the power scale. For simplicity we illustrate the concept of MPM in integral (continuous) form which can be presented as follows:

$$A_{h,\tau_w}^{\text{STFT}}(t',f) = \sqrt{P_{h,\tau_w}^{\text{STFT}}(t',f)} \quad (7a)$$

$$P_{h,\tau_w}^{\text{STFT}}(t',f) = \check{Y}_{h,\tau_w}(t',f) \cdot \check{Y}_{h,\tau_w}^*(t',f) \quad (7b)$$

$$\check{Y}_{h,\tau_w}(t',f) = \tilde{S}_{t',f}^{h,\tau_w}\{y(t)\} = \tilde{\mathcal{F}}_f\{h_{\tau_w,t'} \star y\} \quad (7c)$$

$$\tilde{\mathcal{F}}_f\{x(t)\} = \langle x, e_f \rangle \quad (7d)$$

where $A_{h,\tau_w}^{\text{STFT}}$ is the amplitude of STFT power spectrum $P_{h,\tau_w}^{\text{STFT}}$ of the signal, $\tilde{S}_{t',f}^{h,\tau_w}\{\cdot\}$ is a linear operator of continuous Short-Time Fourier transform, $h_{\tau_w}(t_c|t)$ is a time function of the kernel in the convolution integral which determines the position of the moving data window by its center position t_c , half-length τ_w and shape, $\tilde{\mathcal{F}}_f\{\cdot\}$ is a linear operator of integral (continuous) Fourier transform. The latter can be formulated as an inner product $\langle \cdot, \cdot \rangle$ of the vector of some analyzed function $x(t)$ on space of square integrable functions $L^2(\mathbb{R})$ and of orthogonal basis vectors $e_f = e^{-i2\pi ft}$ supported on $(-\infty, +\infty)$ time interval.

[51] In this work we used a Dolph-Chebyshev time window of two half-widths $\tau_w = 800$ years and $\tau_w = 1600$

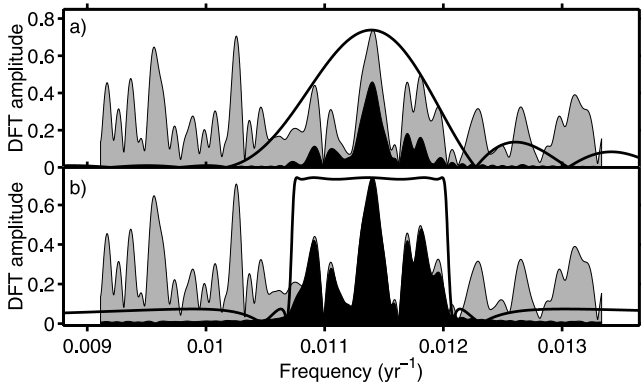


Figure 6. Fourier spectra of raw (light gray profile) and of bandpass filtered (black profiles) $\Delta^{14}C_{atm}^{detr}(t)$ variations, and the filter gains (thick lines) for: a) FIR bandpass filter and b) IIR bandpass filter.

years, and parameter $\alpha = 70$ with amplitude frequency response defined as follows:

$$G_{\alpha}^{Ch}(f) = \frac{\cos\left[\left(\frac{f}{\Delta t} - 1\right) \cdot \arccos\left(\alpha \cos\frac{2\pi f \Delta t}{2}\right)\right]}{\cosh\left[\left(\frac{f}{\Delta t} - 1\right) \cdot \operatorname{arccch}(\alpha)\right]}, \alpha > 0 \quad (8)$$

Our choice of this window kernel was based on the optimal property of its weighting resulting in the minimum window

mainlobe width for a given sidelobe level. Consequently, the Dolph-Chebyshev kernel $h_{Ch}(\tau)$ is determined by Inverse Fourier Transform (IFT).

[52] The 3D-spectrograms of detrended radiocarbon variations $\Delta^{14}C_{atm}^{detr}(t)$ for time interval 9905 B.C.–1895 A.D. for two values of the Dolph-Chebyshev window half-width (800 and 1600 years) within the spectral band around f_G are depicted in Figure 8. In first case (Figure 8a) we have better time resolution and less time-axis end cutoff and in the second case (Figure 8b) we sacrifice the time resolution (becoming twice as wide) and time-axis end regions for greater stability and better frequency resolution. Nevertheless, the both graphs exhibit similar features as follows. The evolution in time of the spectral peak corresponding to the Gleissberg cycle is represented in the frequency–time–amplitude space by a well pronounced ridge going from left to right through all the graph along the time axis. Manifesting undoubtedly the persistence of the cycle through time, yet the ridge does not conservatively preserve its shape. Its crest (marked by dots) varies with ascending and descending waves having its major elevation area for the time interval between ca. 7000 and ca. 1000 B.C. Two profound minima in the Gleissberg peak’s crest elevation are noticeable at the ca. millennia-long intervals centered at ca. 7500 B.C. and ca. 1000 B.C. There is another rising of the ridge at epoch between ca. 12,000–8000 B.C. but this feature can be explained by lower quality of the data in the time series (see discussion above). The crest elevation resumes ascending at modern times around 1000 B.C.

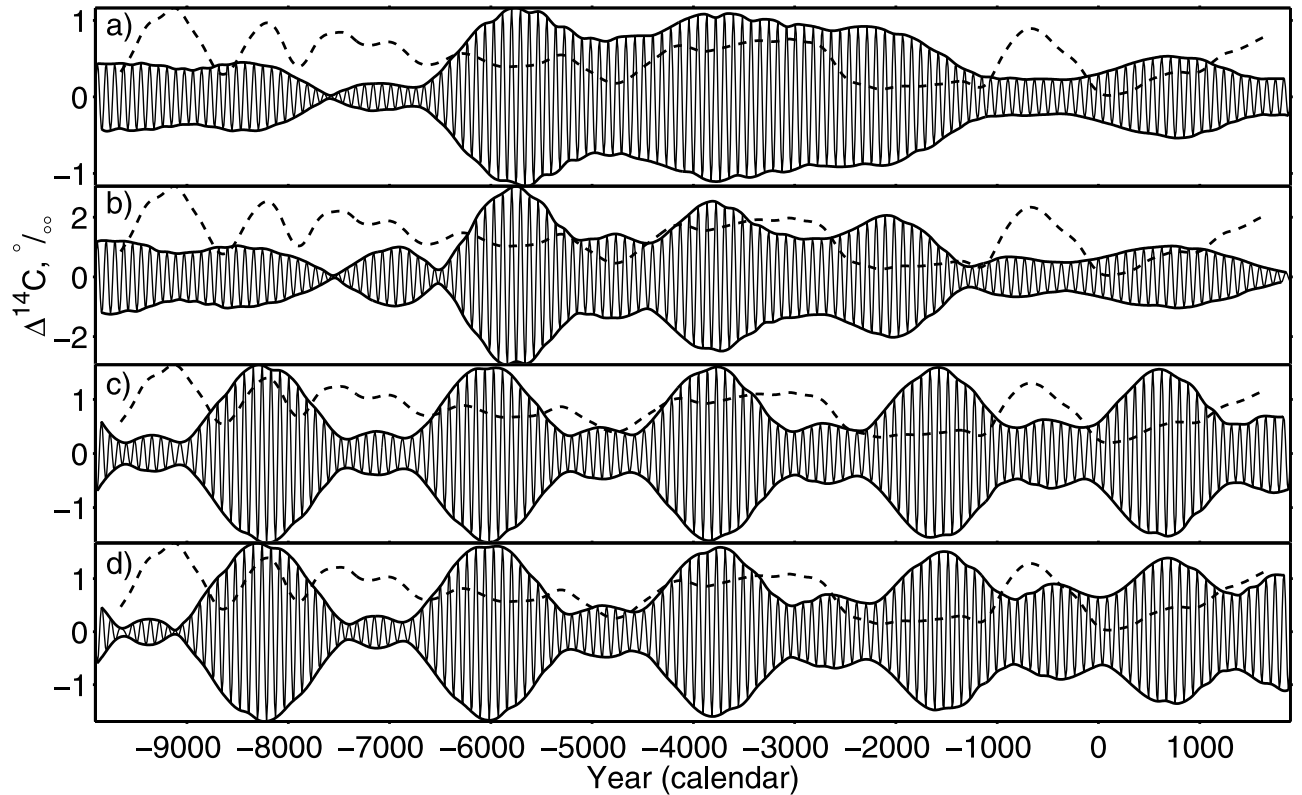


Figure 7. Bandpass filtered $\Delta^{14}C_{atm}$ variations by FIR filter (a) and by IIR filter (b), and harmonic analysis for 3 harmonics: c) for “as is” lines and d) obtained from averaged over 3 spectra. Moving variance variation of original $\Delta^{14}C_{atm}^{detr}$ signal (dashed line) is standardized to the envelopes of all signals (thick line).

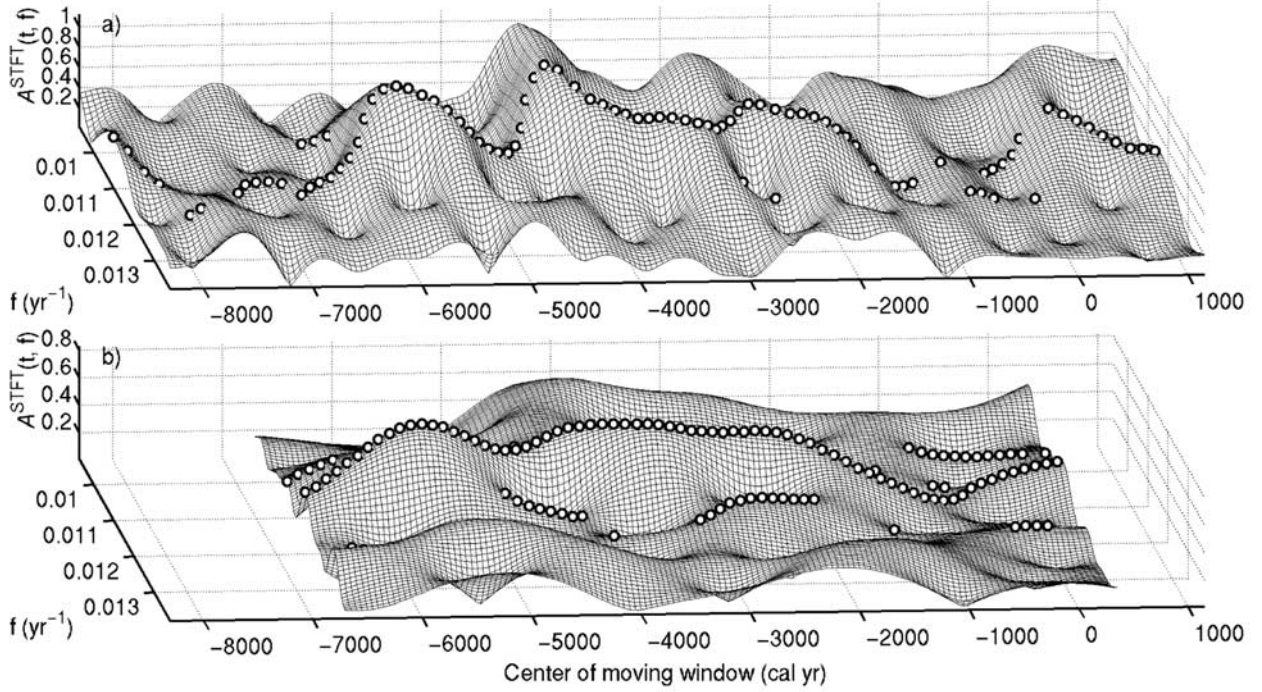


Figure 8. Time–frequency spectrum (spectrogram) of $\Delta^{14}\text{C}_{\text{atm}}^{\text{detr}}$ variations in INTCAL98 record (3D mesh surface of $\sqrt{p_{h_{\tau_w}}^{\text{STFT}}(t, f)}$ for two different half-widths of moving Dolph-Chebyshev window: a) $\tau_w = 800$ years, b) $\tau_w = 1600$ years.

[53] It is of great importance to investigate through different ways of representation the time behavior of the amplitude of the Gleissberg periodicity $A_{88}(t)$. That was done in Figure 9 where the time dependence of the envelopes of the 88-year-centered bandpass filtered (FIR and IIR) time variations from Figures 7a–7b and the height of the crest of the 88-year time–frequency ridge for moving window $L = 3200$ years from Figure 8b were depicted on the same axes. One can notice remarkable matching of the main features among all curves. All curves exhibit remarkable major rise between ca. 7000 B.C. and ca. 700 B.C. Before and after these points all series demonstrate some elevation toward the ends of the whole time interval except the right-hand end of the envelope of the IIR-bandpass filtered variations. Also we should note that the envelope of the FIR-bandpass filtered variations and the height of the crest of the 88-year ridge in spectrogram match each other in concordant manner.

[54] Beside the major trend they experience another variation of oscillatory character which we can interpret through mere visual analysis as a quasiperiodic process of the period in the range of ~ 2000 – 2500 years. That perception is strongly supported by the Fourier analysis (DFT) of residual variations after long-term trends obtained by smoothing spline $\tilde{\mathcal{H}}_{\text{Spl}(6 \cdot 10^3, 0.95)}\{\cdot\}$ were subtracted from the considered estimates of the amplitude of the 88-year cycle $A_{88}(t)$:

$$A_{88}^{\text{detr}}(t) = A_{88}(t) - \tilde{\mathcal{H}}_{\text{Spl}(6 \cdot 10^3, 0.95)}\{A_{88}(t)\} \quad (9)$$

The spectra (which we do not present) not only confirmed the presence of an obvious dominant cycle of almost perfect

shape but also provided estimates of the period equal to 2089 and 2092 years from the envelopes of filtered variations and 2051 years from the height of the 88-years crest on the spectrogram. That result is not surprising at all because above we have already been able to detect the amplitude modulation of the 88-year cycle by ~ 2200 -year periodicity in indirect way through its manifestation in frequency domain (Figures 5 and 6). Now it is detected directly and we can estimate the magnitude of the effect.

[55] At this moment it is difficult to make resolved choice between different causes of the major modulation. Although, the hypothesis of the variation of solar dynamo looks more plausible because we can likely rule out the cause of climate. The climatic series, especially $\delta^{18}\text{O}$ series, do not exhibit any special peculiarities in their time behavior during those time intervals around ~ 7000 B.C. and ~ 700 B.C.

6. Implications of the Gleissberg Cycle for the Theories of Solar Dynamo and Solar Forcing of Climate

[56] *Sonett* [1982] demonstrated that the square law of the Hale magnetic 22-year cycle modulated by 90-year Gleissberg cycle could account for all features of the power spectrum of the Wolf sunspot number index providing that a small offset is included in the Hale carrier. According to Sonett, “the offset suggests a small relict magnetic field in solar core”.

[57] *Feynman and Gabriel* [1990] considered the 88-year cycle to be a subharmonic of the 11-year cycle as a result of triple doubling of the period with the second doubling being

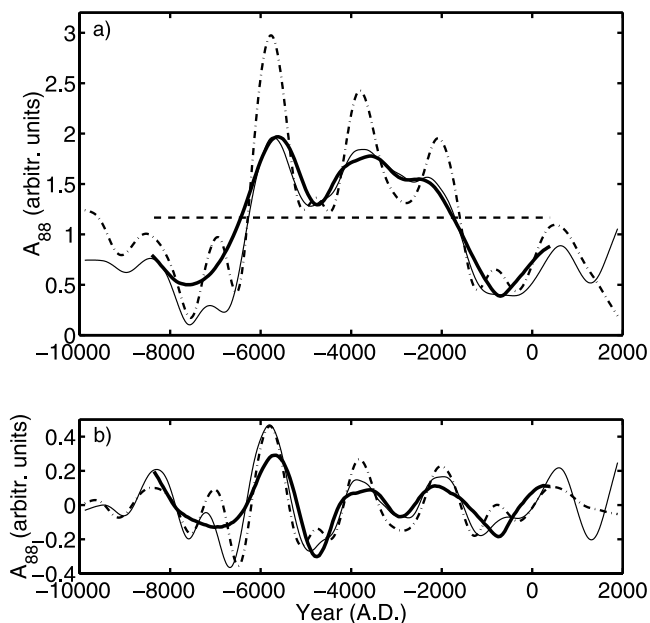


Figure 9. Time variation of the amplitude of the Gleissberg cycle in $\Delta^{14}\text{C}$ data derived from: envelope of the FIR bandpass filtered $\Delta^{14}\text{C}_{\text{atm}}$ (thin line), envelope of the IIR bandpass filtered $\Delta^{14}\text{C}_{\text{atm}}$ (broken line); height of the crest of the 88-year ridge in spectrogram (thick line) and its average level (dashed line), a) raw variation, b) residual variation after removing trend obtained by smoothing spline $\mathcal{H}_{\text{Spl}(6000,0.95)}\{\cdot\}$ and standardization.

weak. According to the authors, this indicates “that the solar dynamo is chaotic and is operating in a region close to the transition between period doubling and chaos”. *Attolini et al.* [1990] also suggested the 88-year cycle to be a subharmonic of the 22-year Hale cycle.

[58] In recent years the problem of the origin of a long secular cycle modulating the sunspot cycle in processes of the solar dynamo has drawn significantly more attention of theoretical solar physicists. After successful demonstration of natural occurrence of aperiodically modulated oscillations in nonlinear hydromagnetic dynamos by *Weiss et al.* [1984] more efforts were directed into this research. *Tobias* [1996] succeeded to reproduce the modulation of the basic 11-year cycle in a nonlinear $\alpha\omega$ dynamo model. He maintained that in the limit of small magnetic Prandtl number τ the ratio of the period of modulation to the basic cycle related as $\propto \tau^{-1/2}$. In another work *Tobias* [1997] introduced two mechanisms of producing modulation of the basic 11-year cycle to the model with a sufficiently realistic nonlinearity. They included modulation of the toroidal magnetic field energy associated with large changes in the parity of the solutions and modulation of the magnetic field by including the action of the Lorenz force in driving plasma velocity perturbations as in the Malkus-Proctor mechanism.

[59] *Pipin* [1999] explored further the problem of theoretical explanation of the Gleissberg cycle. Some magnetohydrodynamic scenarios were simulated to obtain a solution of long-term secular variation within the frame-

work of modern 2D theories of solar dynamo. A long cycle was suggested to be the result of the magnetic feedback on angular momentum fluxes driving the differential rotation in the spherical shell of the convection zone in a 2D model of a distributed dynamo (weak nonlinear $\alpha\Lambda$ dynamo). In contrast to the interface dynamo where the long period is dependent on the effective magnetic Prandtl number P_m as $P_m^{-1/2}$ the approach in this paper did not reveal any such dependence. Rather than that the period of the long cycle was found to be a universal value in the model. It should be noted that the approach used was the mean-field one which was implemented on the basis of the quasi-linear approximation. The long-term variations of the surface angular momentum were found to lag behind magnetic activity variations by two short cycles (or one magnetic cycle). An important feature of the modeled cycle is its relaxation origin. *Pipin* also found that under some conditions the long cycle period can double which we can interpret as promising in regard to possibility of explanation of the “double secular” or Suess cycle. However, it must be pointed out that the considered model bears a number of simplifying assumptions, and one of them is restricted weakness of nonlinearity.

[60] In another work *Saar and Brandenburg* [1999] studied nondimensional relationships between the magnetic dynamo cycle period P_{cyc} , the rotational period P_{rot} , the activity level (mean fractional Ca II H and K flux) and other stellar properties derived from observational data of stellar astronomy. The authors have confirmed the previous finding by *Brandenburg et al.* [1998] that the population of the most stars with age $t \gtrsim 0.1$ Gyr can be split into subpopulations occupying two roughly parallel branches on a diagram $\log \omega_{\text{cyc}}/\Omega_{\text{rot}}$ versus $\log Ro$ where Ro is the Rossby number. The second (“active” or A) branch of stellar population in their survey corresponds to the population of stars with much longer period of the activity cycles (by factor of ~ 6) than the stars of the first (“inactive” or I) branch. They related that timescale of activity to Gleissberg-like periods and suggested that the existence of different branches can correspond to different metastable attractors.

[61] The importance of the Gleissberg cycle is increased also by its significance in studies of solar–terrestrial connections. It is not our intention to discuss in detail the role of the Gleissberg cycle in climate change. Prior to NASA’s Solar Maximum Mission satellite instrumental (ACRIM/I) monitoring of solar irradiance [*Willson and Hudson*, 1991] it was popular to refer to the “solar constant”. Suggestions of a role of the Sun in climate change were frequently not taken seriously or even ridiculed because of the excesses of the Schwabe cycle correlations sometimes referred to as “cyclomania”. However, since the demonstration of a ca. 0.1% change in solar irradiance during the NASA mission, the role of the Sun has been taken seriously leading to many publications. That was essentially initiated by *Eddy* [1976] who suggested “a possible relationship between the overall envelope of the curve of solar activity and terrestrial climate” found from comparison between sunspot number and climatic records. That logically lead him to conclusion that “the long-term envelope of sunspot activity carries the indelible signature of slow changes in solar radiation” [ibid.].

[62] Eventually, the implicit assumption has become that there is an irradiance component accompanying solar activity that varies with the century-scale cycle. For example, *Reid and Gage* [1988] suggested that there is a component of solar luminosity variability associated with the quasi-sinusoidal Gleissberg cycle. In that perspective they performed an analysis of average sea-surface temperatures (SST). The authors concluded that modulation of the Sun's luminosity with a period of about 80 years and an amplitude of about 0.5% was consistent with the globally averaged direct SST measurements. That study was developed further by *Reid* [1991] who demonstrated a good correlation with some lag between eleven-year running means of the Zürich sunspot number and global average SST anomalies. Therefore the envelope of the 11-year sunspot cycle was used for modeling SST variations that again showed good correlation between observed and reconstructed variations. Unfortunately, the required estimates of the solar irradiance at the level of 1% are too high to explain the terrestrial temperatures for a time period since mid-seventeen century exclusively by solar forcing according to observations and models provided by solar physics [*Sofia et al.*, 1979; *Sofia*, 1998]. The difficulty of such "simplistic" approach was emphasized again by *Reid* [1991] who noted that solar variability might not be the only contributor to climate change but "the growing atmospheric burden of greenhouse gases may well have played an important role in the immediate past".

[63] Nevertheless, new attempts have been made to explain the total 20th century warming by changes in solar activity alone. For example, *Friis-Christensen and Lassen* [1991, 1994] has been used variations of solar cycle length to explain the total 20th century warming. As has been noticed by *Damon and Peristykh* [1999] this is again equivalent to climate change forcing by variations of the Gleissberg cycle timescale. This not only requires excessive solar forcing by the Gleissberg cycle but also repetitive global warming of similar magnitude in the past 300 years (see Figure 2b) which is not in accord with paleoclimatological data [*Mann et al.*, 1998; *Damon and Peristykh*, 1999].

7. Conclusions

[64] As well known, the Gleissberg cycle is manifested both in amplitude and period of the Schwabe cycle determined from relative sunspot numbers during the last 300 years. The fitting of the period of the Gleissberg cycle in modulated sunspot number time series yields a value very close to 88 years as in aurora sightings time series.

[65] The Gleissberg cycle is prominent in Fourier spectra of cosmogenic isotopes variations in the Earth's atmosphere (INTCAL98 radiocarbon record) for the last $\sim 11,854$ years. The period of the Gleissberg cycle determined from long records of cosmogenic isotope data is equal to 88 ± 0.2 years. We confirmed that the Gleissberg cycle is modulated by the 208-year Suess cycle which is manifested and justified by their combination tones. The periods of those tones as we determined from the new, improved data set are ~ 150 and ~ 61 years.

[66] We found that the amplitude of the Gleissberg cycle appears to be modulated by a long-term quasiperiodic process of timescale ~ 2200 years. This can be detected

indirectly by their combination tones at periods $\approx 91.5 \pm 0.1$ and $\approx 84.6 \pm 0.1$ years. Although this may be an oversimplification because more than one sideband of 88-year peak can be observed in frequency domain in Figure 5 and Figure 6. Thus, other long-term processes may be involved in modulation of the Gleissberg cycle.

[67] Also there is other, direct, evidence observed in time domain for modulation of the Gleissberg cycle magnitude by a long-term process of ca. 2000-year timescale as revealed by bandpass filtering and time-frequency analysis of the INTCAL98 radiocarbon record (Figures 7a–7b and 9).

[68] As a closing remark, we would like to point out that revealing the apparent stability of the Gleissberg cycle over such a long period of time is of interest and of great significance for solar physics and presents an interesting challenge to solar dynamo theories. That stability may also possibly set limits on quasi-chaotic behavior of solar processes on longer than 11-year timescales.

[69] **Acknowledgments.** This work was completed under National Science Foundation Grant ATM-9819228.

References

- Ahmad, I., G. Bonino, G. Cini Castagnoli, S. M. Fischer, W. Kutschera, and M. Paul, Three-laboratory measurement of the ^{44}Ti half-life, *Phys. Rev. Lett.*, **80**, 2550–2553, 1998.
- Attolini, M. R., S. Cecchini, and M. Galli, Time series variation analysis with Fourier vector amplitudes, *Nuovo Cimento Soc. Ital. Fis. C*, **7**, 245–253, 1984.
- Attolini, M. R., M. Galli, and G. Cini Castagnoli, On the R(z)-sunspot relative number variations, *Sol. Phys.*, **95**, 391–395, 1985.
- Attolini, M. R., S. Cecchini, M. Galli, and T. Nanni, The Gleissberg and 130 year periodicity in the cosmogenic isotopes in the past: The Sun as a quasi-periodic system, in *Proceedings of the 20th International Cosmic Ray Conference, Moscow*, vol. 4, p. 323, Nauka, Moscow, 1987.
- Attolini, M. R., M. Galli, and T. Nanni, Long and short cycles in solar activity during the last millennia, in *Secular Solar and Geomagnetic Variations in the Last 10,000 Years*, edited by F. R. Stephenson and A. W. Wolfendale, pp. 49–68, Kluwer Acad, Norwell, Mass., 1988.
- Attolini, M. R., S. Cecchini, M. Galli, and T. Nanni, On the persistence of the 22-year solar cycle, *Sol. Phys.*, **125**, 389–398, 1990.
- Bhandari, N., G. Bonino, E. Callegari, G. Cini Castagnoli, K. Mathew, J. Padia, and G. Queirazza, The Torino, H6, meteorite shower, *Meteoritics*, **24**, 29–34, 1989.
- Bonino, G., Measurement of ^{44}Ti (^{44}Sc) in meteorites, *Nuovo Cimento Soc. Ital. Fis. C*, **16**, 29–33, 1993.
- Bonino, G., G. Cini Castagnoli, C. Taricco, and N. Bhandari, Cosmogenic ^{44}Ti in meteorites and century scale solar modulation, *Adv. Space Res.*, **14**, 783–786, 1994.
- Bonino, G., G. Cini Castagnoli, N. Bhandari, and C. Taricco, Behavior of the heliosphere over prolonged solar quiet periods by ^{44}Ti measurements in meteorites, *Science*, **270**, 1648–1650, 1995a.
- Bonino, G., G. Cini Castagnoli, N. Bhandari, and C. Taricco, Titanium-44 in meteorites: Evidence for a century-scale solar modulation of galactic cosmic rays, *Meteoritics*, **30**, 489, 1995b.
- Bonino, G., G. Cini Castagnoli, C. Taricco, P. della Monica, and N. Bhandari, Decadal and century scale modulation of cosmogenic radionuclides measured in meteorites, *Meteorit. Planet. Sci.*, **32**, A17, 1997.
- Bonino, G., G. Cini Castagnoli, P. della Monica, C. Taricco, and N. Bhandari, Heliospheric behavior in the past by titanium-44 measurement in chondrites, *Meteorit. Planet. Sci.*, **33**, A19, 1998.
- Bonino, G., G. Cini Castagnoli, D. Cane, C. Taricco, and N. Bhandari, Cosmogenic ^{44}Ti in chondrites and galactic cosmic ray variations since the Maunder Minimum, *Meteorit. Planet. Sci.*, **36**, A24, 2001.
- Bonino, G., G. Cini Castagnoli, C. Taricco, N. Bhandari, and M. Killgore, Cosmogenic radionuclides in four fragments of the Portales Valley meteorite shower: Influence of different element abundances and shielding, *Adv. Space Res.*, **27**, 777–782, 2002.
- Brandenburg, A., S. H. Saar, and C. R. Turpin, Time evolution of the magnetic activity cycle period, *Astrophys. J.*, **498**, L51–L54, 1998.
- Cadzow, J. A., *Foundations of Digital Signal Processing and Data Analysis*, Macmillan, Old Tappan, N. J., 1987.

- Cini Castagnoli, G., G. Bonino, and A. Provenzale, The thermoluminescence profile of a recent sea sediment core and the solar variability, *Sol. Phys.*, 117, 187–197, 1988.
- Cini Castagnoli, G., G. Bonino, and A. Provenzale, The 206-year cycle in tree ring radiocarbon data and in the thermoluminescence profile of a recent sea sediment, *J. Geophys. Res.*, 94, 11,971–11,976, 1989.
- Cini Castagnoli, G., G. Bonino, M. Serio, and C. P. Sonett, Common spectral features in the 5500-year record of total carbonate in sea sediments and radiocarbon in tree rings, *Radiocarbon*, 34, 798–805, 1992.
- Cini Castagnoli, G., G. Bonino, and C. Taricco, Solar magnetic and bolometric cycles recorded in sea sediments, *Sol. Phys.*, 152, 309–312, 1994.
- Damon, P. E., and A. N. Peristykh, Solar cycle length and 20th century Northern Hemisphere warming: Revisited, *Geophys. Res. Lett.*, 26, 2469–2472, 1999.
- Damon, P. E., and A. N. Peristykh, Radiocarbon calibration and application to geophysics, solar physics, and astrophysics, *Radiocarbon*, 42, 137–150, 2000.
- Damon, P. E., and C. P. Sonett, Solar and terrestrial components of the atmospheric ^{14}C variation spectrum, in *The Sun in Time*, edited by C. P. Sonett, M. S. Giampapa, and M. S. Matthews, pp. 360–388, Univ. of Ariz. Press, Tucson, 1991.
- Damon, P. E., J. C. Lerman, and A. Long, Temporal fluctuations of atmospheric ^{14}C : Causal factors and implications, *Annu. Rev. Earth Planet. Sci.*, 6, 457–494, 1978.
- de Vries, H., Variation in concentration of radiocarbon with time and location on Earth, *Proc. K. Ned. Akad. Wet., Ser. B*, 61, 94–102, 1958.
- Dewey, E. R., The length of the sunspot cycle, *J. Cycle Res.*, 7, 79–91, 1958.
- Dmitriev, P. B., A. N. Peristykh, and A. A. Kharchenko, The variations of radiocarbon content in the Earth's atmosphere over AD 1600–1730, *Prepr. No.1104*, A. F. Ioffe Inst. of Phys. and Technol., USSR Acad. of Sci., Leningrad, 1987.
- Eddy, J. A., The last 500 years of the Sun, in *Proceedings of the Workshop "The Solar Constant and the Earth's Atmosphere"*, 19–21 May 1975, edited by H. Zirin and J. Walter, pp. 98–108, Big Bear Sol. Observ., Big Bear City, Calif., 1975.
- Eddy, J. A., The Maunder Minimum, *Science*, 192, 1189–1202, 1976.
- Eddy, J. A., Historical evidence for the existence of the solar cycle, in *The Solar Output and Its Variation*, edited by O. R. White, pp. 51–71, Colo. Assoc. Univ. Press, Boulder, Colo., 1977.
- Elsasser, W., E. P. Ney, and J. R. Winckler, Cosmic-ray intensity and geomagnetism, *Nature*, 178, 1226–1227, 1956.
- Emilio, M., J. R. Kuhn, R. I. Bush, and P. Scherrer, On the constancy of the solar diameter, *Astrophys. J.*, 543, 1007–1010, 2000.
- Feynman, J., Solar wind variations in the 60–100 year period range: A review, in *5th Solar Wind Conference*, pp. 333–345, NASA, Washington, D.C., 1983.
- Feynman, J., and P. F. Fougere, Eighty-eight year periodicity in solar-terrestrial phenomena confirmed, *J. Geophys. Res.*, 89, 3023–3027, 1984.
- Feynman, J., and S. B. Gabriel, Period and phase of the 88-year solar cycle and the Maunder minimum: Evidence for a chaotic Sun, *Sol. Phys.*, 127, 393–403, 1990.
- Friis-Christensen, E., and K. Lassen, Length of the solar cycle: An indicator of solar activity closely associated with climate, *Science*, 254, 698–700, 1991.
- Friis-Christensen, E., and K. Lassen, Solar activity and global climate, in *The Sun as a Variable Star: Solar and Stellar Irradiance Variations*, edited by J. M. Pap. C. Fröhlich, H. S. Hudson, and S. K. Solanki, pp. 339–347, Cambridge Univ. Press, New York, 1994.
- Gilliland, R. L., Solar radius variations over the past 265 years, *Astrophys. J.*, 248, 1144–1155, 1981.
- Giordano, A. A., and F. M. Hsu, *Least Square Estimation With Applications to Digital Signal Processing*, John Wiley, New York, 1985.
- Gleissberg, W., A table of secular variations of the solar cycle, *Terr. Magn. Atmos. Electr.*, 49, 243–244, 1944.
- Gleissberg, W., The eighty-year sunspot cycle, *J. Br. Astron. Assoc.*, 68, 148–152, 1958.
- Gleissberg, W., The eighty-year solar cycle in auroral frequency numbers, *J. Br. Astron. Assoc.*, 75, 227–231, 1965.
- Gleissberg, W., Ascent and descent in the eighty-year cycles of solar activity, *J. Br. Astron. Assoc.*, 76, 265–268, 1966.
- Gleissberg, W., Secularly smoothed data on the minima and maxima of sunspot frequency, *Sol. Phys.*, 2, 231–233, 1967.
- Gleissberg, W., Das jüngste Maximum des achtzigjährigen Sonnenfleckenzyklus, *Kleinheub. Ber.*, 19, 661–664, 1976.
- Honda, M., and J. R. Arnold, Effects of cosmic rays on meteorites, *Science*, 143, 203–212, 1964.
- Kocharov, G. E., and A. N. Peristykh, Time–frequency analysis of data on solar activity and solar–terrestrial relations over the past 400 years (in Russian), in *Potentialities of the Measurement Methods for Isotopes of Super-Low Abundance*, edited by G. E. Kocharov, pp. 5–27, A. F. Ioffe Inst. of Phys. and Technol., USSR Acad. of Sci., Leningrad, 1990.
- Kocharov, G. E., and A. N. Peristykh, Moving periodogram analysis of data on solar activity and solar–terrestrial relations over the last 400 years, *Soln. Dannye*, 107–115, (in Russian), 1991.
- Kopecký, M., Periodicity of the number of originated sunspot groups and of their average life time, and evaluation of the method of their computation, *Bull. Astron. Inst. Czechoslov.*, 11, 35–52, 1960.
- Kopecký, M., Physical interpretation of the 80-year period of solar activity, *Bull. Astron. Inst. Czechoslov.*, 13, 240–245, 1962.
- Kopecký, M., On the question of the reality of an 80-year period of the average importance of sunspot groups, *Bull. Astron. Inst. Czechoslov.*, 15, 44–48, 1964.
- Kopecký, M., When did the maximum of the present 80-year sunspot period occur?, *Bull. Astron. Inst. Czechoslov.*, 27, 273–275, 1976.
- Kopecký, M., When did the latest minimum of the 80-year sunspot period occur?, *Bull. Astron. Inst. Czechoslov.*, 42, 158–160, 1991.
- Kopecký, M., G. V. Kuklin, and B. Růžičková-Topolová, On the relative inhomogeneity of long-term series of sunspot indices, *Bull. Astron. Inst. Czechoslov.*, 31, 267–283, 1980.
- Lal, D., and B. Peters, Cosmic ray produced radioactivity on the Earth, in *Handbuch der Physik*, edited by K. Sitte, vol. 46/2, pp. 551–612, Springer-Verlag, New York, 1967.
- Libby, W. F., *Radiocarbon Dating*, 2nd ed., Univ. of Chicago Press, Chicago, Ill., 1955.
- Lin, Y. C., C. Y. Fan, P. E. Damon, and E. I. Wallick, Long-term modulation of cosmic-ray intensity and solar activity cycles, in *14th International Cosmic Ray Conference, Munchen*, vol. 3, pp. 995–999, Max-Planck-Institut für extraterrestrische Physik, Garching, Germany, 1975.
- Link, F., Variations à longues périodes de l'activité solaire avant le 17ème siècle, *Bull. Astron. Inst. Czechoslov.*, 14, 226–231, 1963.
- Mann, M., R. Bradley, and M. Hughes, Global-scale temperature patterns and climate forcing over the past six centuries, *Nature*, 392, 779–787, 1998.
- McKinnon, J. A., Sunspot Numbers: 1610–1985, World Data Center A for Sol. Terr. Phys., Boulder, Colo., 1987.
- Merrill, R., M. McElhinny, and P. McFadden, *The Magnetic Field of the Earth: Paleomagnetism, the Core, and the Deep Mantle*, Academic, San Diego, Calif., 1996.
- Michel, R., P. Dragovitsch, P. Cloth, G. Dagge, and D. Filges, On the production of cosmogenic nuclides in meteoroids by galactic protons, *Meteoritics*, 26, 221–242, 1991.
- Mordvinov, A. V., Time–frequency analysis of the Wolf sunspot numbers, *Res. Geomag. Aeron. Sol. Phys.*, 83, 134–141, (in Russian), 1988.
- Neumann, S., I. Leya, and R. Michel, The influence of solar modulation on short-lived cosmogenic nuclides in meteorites with special emphasize on titanium-44, *Meteorit. Planet. Sci.*, 32, A98, 1997.
- Peristykh, A. N., Temporal–spectral characteristics of data on solar activity and on solar–terrestrial relations over the last 400 years, in *Proceedings of the 1st Conference Young Scientists: Physics*, edited by Zh.S. Takibaev, p. 45, Kazakh State Univ., Alma-Ata, 1990.
- Peristykh, A. N., On frequency modulation of the Schwabe cycle of solar activity by longer cycles, *Eos Trans. AGU*, 74, 491, supplement, 1993.
- Peristykh, A. N., Aa-index as an indicator of amplitude and frequency modulation of 11-year solar activity cycle, in *XXI General Assembly of the International Union of Geodesy and Geophysics, Boulder, July 2–14, 1995*, vol. A, p. 158, AGU, Washington, D.C., 1995.
- Pipin, V. V., The Gleissberg cycle by a nonlinear $\alpha\Lambda$ dynamo, *Astron. Astrophys.*, 346, 295–302, 1999.
- Raisbeck, G. M., F. Yiou, J. Jouzel, and J. R. Petit, ^{10}Be and ^6H in polar ice cores as a probe of the solar variability's influence on climate, in *The Earth's Climate and Variability of the Sun Over Recent Millennia: Geophysical, Astronomical and Archaeological Aspects*, edited by J.-C. Pecker and S. K. Runcorn, pp. 65–71, R. Soc., London, 1990.
- Reid, G. C., Solar total irradiance variations and the global sea surface temperature record, *J. Geophys. Res.*, 96, 2835–2844, 1991.
- Reid, G. C., and K. S. Gage, The climatic impact of secular variations in solar irradiance, in *Secular Solar and Geomagnetic Variations in the Last 10,000 Years*, edited by F. R. Stephenson and A. W. Wolfendale, pp. 225–243, Kluwer Acad., Norwell, Mass., 1988.
- Rubashev, B. M., *Problems of Solar Activity (in Russian)*, Acad. of Sci. of the USSR Publ., Moscow-Leningrad, 1964.
- Saar, S. H., and A. Brandenburg, Time evolution of the magnetic activity cycle period, 2, Results for an expanded stellar sample, *Astrophys. J.*, 524, 295–310, 1999.
- Schöve, D. J., The sunspot cycle, 649-BC to AD-2000, *J. Geophys. Res.*, 60, 127–146, 1955.
- Siscoe, G. L., Evidence in the auroral record for secular solar variability, *Rev. Geophys.*, 18, 647–658, 1980.

- Sofia, S., Solar variability and climate change, in *Solar Electromagnetic Radiation Study for Solar Cycle 22*, edited by J. M. Pap, C. Fröhlich, and R. K. Ulrich, pp. 413–418, Kluwer Acad., Norwell, Mass., 1998.
- Sofia, S., J. O’Keefe, J. R. Lesh, and A. S. Endal, Solar constant: Constraints on possible variations derived from solar diameter measurements, *Science*, 204, 1306–1308, 1979.
- Sofia, S., P. Demarque, and A. Endal, From solar dynamo to terrestrial climate, *Am. Sci.*, 73, 326–333, 1985.
- Sonett, C. P., Sunspot time series: Spectrum from square law modulation of the Hale cycle, *Geophys. Res. Lett.*, 9, 1313–1316, 1982.
- Sonett, C. P., Very long solar periods and the radiocarbon record, *Rev. Geophys.*, 22, 239–254, 1984.
- Sonett, C. P., and S. A. Finney, The spectrum of radiocarbon, in *The Earth’s Climate and Variability of the Sun Over Recent Millennia: Geophysical, Astronomical and Archaeological Aspects*, edited by J.-C. Pecker and S. K. Runcorn, pp. 15–27, R. Soc., London, 1990.
- Stuiver, M., Variations in radiocarbon concentration and sunspot activity, *J. Geophys. Res.*, 66, 273–276, 1961.
- Stuiver, M., Carbon-14 content of 18th- and 19th-century wood, variations correlated with sunspot activity, *Science*, 149, 533–535, 1965.
- Stuiver, M., and T. F. Braziunas, Sun, ocean, climate and atmospheric CO₂: An evaluation of causal and spectral relationships, *Holocene*, 3, 289–305, 1993.
- Stuiver, M., and P. D. Quay, Changes in atmospheric carbon-14 attributed to a variable Sun, *Science*, 207, 11–19, 1980.
- Stuiver, M., et al., INTCAL98 radiocarbon age calibration, 24,000-0 cal BP, *Radiocarbon*, 40, 1041–1083, 1998.
- Suess, H. E., The three causes of the secular C14 fluctuations, their amplitudes and time constants, in *Radiocarbon Variations and Absolute Chronology: Proceedings of the Twelfth Nobel Symposium*, edited by I. U. Olsson, pp. 595–604, Almqvist and Wiksell, Stockholm, 1970.
- Suess, H. E., The radiocarbon record in tree rings of the last 8000 years, *Radiocarbon*, 22, 200–209, 1980.
- Tobias, S. M., Grand minima in nonlinear dynamos, *Astron. Astrophys.*, 307, L21–L24, 1996.
- Tobias, S. M., The solar cycle: Parity interactions and amplitude modulation, *Astron. Astrophys.*, 322, 1007–1017, 1997.
- Vasil’ev, O. B., Time–frequency spectrum of Zurich Wolf number series (1701–1964), *Soln. Dannye*, Solar Data, 92–99, (in Russian), 1970.
- Vitinskii, Y. I., *Solar-Activity Forecasting*, Isr. Program for Sci. Transl., Jerusalem, 1965.
- Vitinskii, Y. I., M. Kopecký, and G. V. Kuklin, *Statistics of the Sunspot Formation Activity of the Sun (in Russian)*, Nauka, Moscow, 1986.
- Vogt, S., G. F. Herzog, and R. C. Reedy, Cosmogenic nuclides in extra-terrestrial materials, *Rev. Geophys.*, 28, 253–275, 1990.
- Weiss, N. O., F. Cattaneo, and C. A. Jones, Periodic and aperiodic dynamo waves, *Geophys. Astrophys. Fluid Dyn.*, 30, 305–341, 1984.
- Willson, R. C., and H. S. Hudson, The Sun’s luminosity over a complete solar cycle, *Nature*, 351, 42–44, 1991.
- Wittmann, A., The sunspot cycle before the Maunder Minimum, *Astron. Astrophys.*, 66, 93–97, 1978.

P. E. Damon and A. N. Peristykh, Department of Geosciences, University of Arizona, Gould-Simpson Building 88, Tucson, AZ 85721, USA. (damon@geo.arizona.edu; peristy@geo.arizona.edu)